*Annals of Biomedical Engineering*, Vol. 39, No. 4, April 2011 (© 2011) pp. 1335–1348
DOI: 10.1007/s10439-011-0270-0

# Activatable $T_1$ and $T_2$ Magnetic Resonance Imaging Contrast Agents

CHUQIAO TU,[1] ELIZABETH A. OSBORNE,[2] and ANGELIQUE Y. LOUIE[1]

[1]Department of Biomedical Engineering, University of California, Davis, CA 95616, USA; and [2]Department of Chemistry, University of California, Davis, CA 95616, USA

(*Received 6 January 2011; accepted 4 February 2011; published online 18 February 2011*)

Associate Editor Daniel Takashi Kamei oversaw the review of this article.

**Abstract**—Magnetic resonance imaging (MRI) has become one of the most important diagnosis tools available in medicine. Typically MRI is not capable of sensing biochemical activities. However, recently emerged activatable MRI contrast agents (CAs), whose relaxivity is variable in response to a specific parameter change in the surrounding physiological microenvironment, potentially allow for MRI to indicate biological processes. Among the various factors influencing the relaxivity of a CA, the number of inner-sphere water molecules ($q$) directly coordinated to the metal center, the residence time of the coordinated water molecule ($\tau_m$), and the rotational correlation time representing the molecular tumbling time of a complex ($\tau_R$) contribute strongly to the relaxivity of an activatable CA. Tuning the ligand structure and properties has been the subject of intensive research for activatable MR CA designs. This review summarizes a variety of activatable MRI CAs sensitive to common variables in microenvironment *in vivo*, i.e., pH, luminescence, metal ions, redox, and enzymes, etc., with emphasis on the influence of ligand design on parameters $q$, $\tau_m$, and $\tau_R$.

**Keywords**—Magnetic resonance imaging (MRI), Contrast agent, Relaxivity, Gadolinium, Activatable, Responsive.

## INTRODUCTION

Since the first inception of X-ray technology for medical imaging over a century ago, many non-invasive imaging methodologies have been developed and applied to biomedical science with the help of the significant advances in electronics, information technology, and nanotechnology.[22,73,86] Today imaging has become an indispensable tool in laboratory research, clinical trials, and medical practice. Because of advantages of high spatial resolution, the best soft-tissue contrast in all currently available imaging modalities, low toxicity, and the absence of ionizing radiation, magnetic resonance imaging (MRI) has been singled out as the *in vivo* diagnostic technology for the next generation.[46,84,88]

MRI provides anatomical images by measuring proton ($^1$H) relaxation processes of water and soft tissues in biological systems.[12] The spinning of the $^1$H nucleus generates a weak magnetic dipole. In thermodynamic state, all the nuclear dipoles are oriented randomly thus the net magnetic moment is zero. When an external field $B_0$ is applied, the $^1$H nuclei experience a torque which forces them "align" with the field in two separate, quantized energy states. The energy difference of the two quantized states ($\Delta E$) is a function of the gyromagnetic ratio of the spin ($\gamma$), reduced Planck's constant ($\hbar$), and external magnetic field ($B_0$) (Eq. 1).

$$\Delta E = \gamma \hbar B_0 \tag{1}$$

The frequency of the energy ($\nu$) (Eq. 2) required for an NMR transition is commonly represented by Larmor frequency ($\omega$) (Eq. 3).

$$\nu = \gamma B_0 / 2\pi \tag{2}$$

$$\omega = 2\pi\nu = \gamma B_0 \tag{3}$$

The energy required for a $^1$H nuclear spin ($\gamma = 42.576$ MHz T$^{-1}$) transition at currently available external fields (up to 15 T) is at the magnitude of $10^{-25}$ J which corresponds to radiowaves in the electromagnetic spectrum. The low energy of NMR means it is a very insensitive technique. When a resonant radio frequency (RF) transverse pulse is perpendicularly applied to $B_0$, it causes resonant excitation of the magnetic moment precession into the perpendicular plane. Once the RF perturbation is removed, the dipoles return or "relax" to thermodynamic

Address correspondence to Angelique Y. Louie, Department of Biomedical Engineering, University of California, Davis, CA 95616, USA. Electronic mail: aylouie@ucdavis.edu
Elizabeth A. Osborne—co-first author.

equilibrium. The relaxation behavior of the dipoles is described by longitudinal $T_1$ relaxation (loss of energy from the excited state to its surroundings, termed as spin–lattice interaction) and transverse $T_2$ relaxation (random variations in local field strength, caused by neighboring spins, de-synchronize the signals, termed as spin–spin interaction).[13]

The signal emitted by the hydrogen nuclei during relaxation is referred to as the *free-induction decay* (FID) response signal. To produce an MRI image, the FID resonance signal must be encoded from each dimension. The encoding in the $Z$ axial direction of $B_0$ is accomplished by adding a gradient magnetic field to $B_0$. The gradient causes the Larmor frequency $\omega$ to change linearly in the $B_0$ direction. A tiny axial slice in that direction is then selected and $\omega$ of hydrogen nuclei in the slice is assumed to be identical. The spatial reconstruction of each axial slice is realized by using frequency and phase encoding. A gradient $G_y$ is applied, causing the resonant frequencies of the nuclei in the slice to vary according to their position in the $Y$ axial direction. $G_y$ is then removed and another gradient $G_x$ is applied perpendicular to $G_y$. As a result, the resonant frequencies of the nuclei vary in the $X$ axial direction due to $G_x$ and have a phase variation in the $Y$ axial direction due to the previously applied $G_y$. Therefore, samples are encoded by frequency in the $X$ axial direction and by phase in the $Y$ axial direction. A Fourier Transform is then used to transform the encoded image to a plane image.[13]

Intensity of signals from each volume element (voxel) of a given tissue type is a function of *proton density* of the tissue. The higher the proton density, the stronger the FID response signal. The MR image contrast also depends on tissue-specific parameters $T_1$ and $T_2$. When MR images are acquired, the RF pulse is repeated at a predetermined rate. The period of the RF pulse sequence is the *repetition time*, *TR*. The time between which the RF pulse is applied and the response signal is measured is the *echo delay time*, *TE*. By adjusting *TR* and *TE* the acquired MR image can possess contrast for different tissue types.[13]

Because the endogenous MR differences among various types of tissues can be small, a contrast agent (CA) is often used in MRI to provide additional contrast to distinguish a target tissue from its surroundings. Clinical CAs are in the form of either paramagnetic gadolinium ($Gd^{3+}$) or manganese ($Mn^{2+}$) chelates, or superparamagnetic iron oxide (SPIO) and ultrasmall superparamagnetic iron oxide (USPIO) nanoparticles that take effect by catalytically shortening the relaxation times of bulk water protons. Paramagnetic chelates increase the longitudinal relaxation rate ($R_1$) by roughly the same extent as that they increase the transverse relaxation rate ($R_2$). They exhibit "positive" (bright) contrast where they localize and are referred to as $T_1$ agents. In contrast to paramagnetic chelates, iron oxide nanoparticles increase the transverse relaxation rate ($R_2$) to a much greater extent than they increase the longitudinal relaxation rate ($R_1$). They exhibit "negative" (dark) contrast where they localize and are referred to as $T_2$ agents.[34]

The proportion of clinical MRI protocols using CAs has increased rapidly, from approximately 30% in 1999 to a current estimation of 40–50%.[16,85] "Positive" CAs generally are more preferable in the clinic compared to those that induce "negative" contrast or signal loss. It is easier to ascribe signal enhancement, rather than signal loss, to CA accumulation in tissue because there are potentially other sources of signal loss in MR images beyond iron oxide nanoparticle accumulation.[25] The majority of MRI CAs currently used in the clinic are chelates of $Gd^{3+}$ ions, as shown in Fig. 1 and Table 1, because the lanthanide ion has a large magnetic moment and long electronic relaxation time, therefore offering excellent "positive" image contrast.[16,38]

The most important property of a CA is its relaxivity ($r$) that reflects the ability of the CA to generate imaging signal contrast. The $r_1$ relaxivity of a CA is the agent's ability to affect the longitudinal relaxation rate $r_1$ ($=1/T_1$) of water protons and its value is expressed in $mM^{-1}\,s^{-1}$.[77] According to the Solomon–Bloembergen–Morgan (SBM) theory, relaxivity originates from the dipole–dipole interactions between the proton nuclear spins and the fluctuating local magnetic field caused by the unpaired electron spins of the paramagnetic substance.[17] Relaxivity depends on a number of factors including the number of inner-sphere water molecules ($q$) directly coordinated to the metal center, the residence time of the coordinated water molecule ($\tau_m$), the rotational correlation time representing the molecular tumbling time of a complex ($\tau_R$), electronic parameters, paramagnetic metal ion-proton distance, external field, and temperature.[15,17,38,77] The water molecules coordinated to the metal center in Gd-based clinical CAs are defined as the inner-sphere or the first-sphere water molecules (Fig. 2). The Gd CAs have typical values of more than 100 ns for $\tau_m$ and 0.1 ns for $\tau_R$, which results in a low $r_1$ relaxivity (~5 $mM^{-1}\,s^{-1}$ at 1.5 T) because the optimal values of these agents at 1.5 T should be approximately 10 ns for $\tau_m$ and at least 10 ns for $\tau_R$ according to SBM theory. The $\tau$ values can be altered via ligand designs that allow faster water exchange and slower molecular tumbling. The tuning of the ligand structure has been the subject of intensive research for the past two decades because an increase in the relaxivity allows for a dramatic decrease in the application dose.[15,26,85,87]

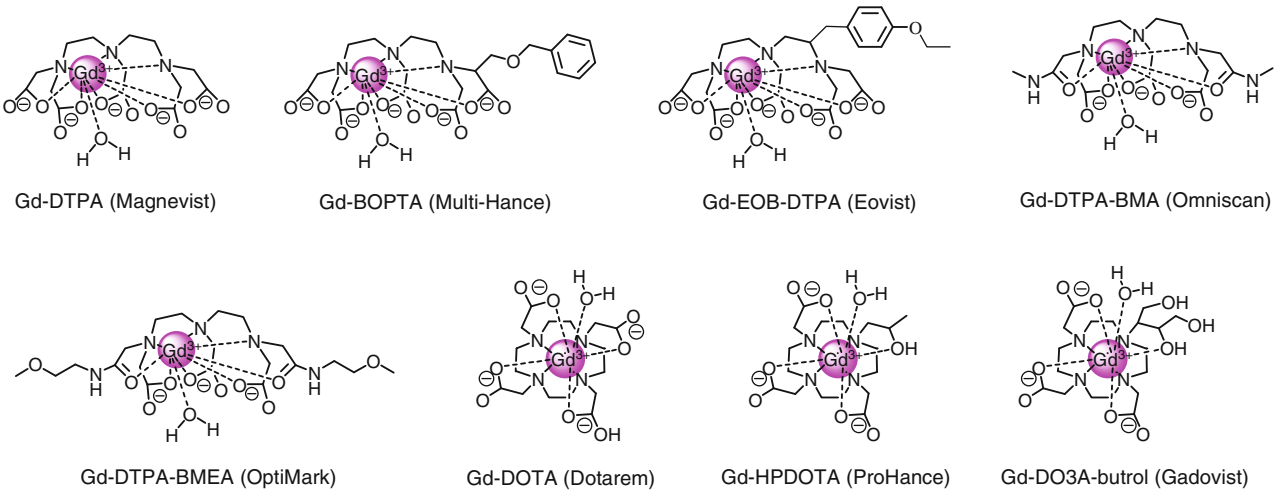


**FIGURE 1. Chemical structures including one coordinated water molecule, chemical names, and trademark names of Gd-based MRI CAs approved for clinical use in the EU and USA.**

**TABLE 1. Properties of clinically approved, Gd-based MRI CAs.[2,85]**

| Trade name | Type | Plasma relaxivity (1.5 T, 37 °C) ($mM^{-1}$ $s^{-1}$) $r_1$ | $r_2$ | Log $K_{ML}$ | Clearance | Osmolality (Osm/kg $H_2O$) | Location |
|---|---|---|---|---|---|---|---|
| Magnevist | Ionic | 4.1 | 4.6 | 22.1 | Renal | 1.96 | EU, USA |
| Omniscan | Neutral | 4.3 | 5.2 | 16.9 | Renal | 0.79 | EU, USA |
| Optimark | Neutral | 4.7 | 5.2 | 16.6 | Renal | 1.11 | EU, USA |
| Dotarem | Ionic | 3.6 | 4.3 | 25.8 | Renal | 1.35 | EU |
| Prohance | Neutral | 4.1 | 5.0 | 23.8 | Renal | 0.63 | EU, USA |
| Gadovist | Neutral | 5.2 | 6.1 | 21.8 | Renal | 1.60 | EU |
| Multihance | Ionic | 6.3 | 8.7 | 22.6 | Renal/Hepatic | 1.97 | EU, USA |
| Envist | Ionic | 6.9 | 8.7 | 23.5 | Renal/Hepatic | 0.69 | EU, USA |

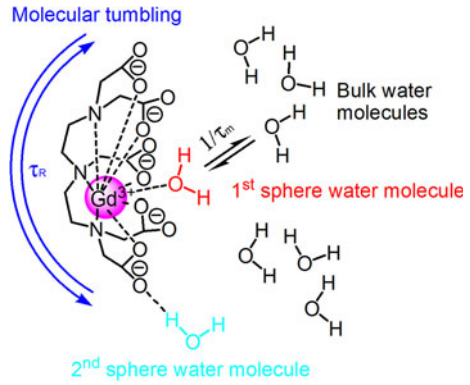


**FIGURE 2. Schematic illustration of molecular parameters influencing relaxivity of Gd-based MRI CAs in solution. Image modified from Fig. 2 in Werner *et al.*.**

Most of clinically approved Gd CAs are extracellular fluid (ECF) MRI CAs. Their low molecular weight allows them to equilibrate rapidly between the intravascular and interstitial space and then clear almost exclusively by renal filtration on the time scale of a few hours. The ECF CAs are generally nonspecific. They do not interact specifically with any type of cells, though their distribution in the body is far from homogeneous.[34] MRI with ECF CAs is typically used for a whole body scan, and is not capable of sensing biochemical activities. During the last decade, new types of CAs have been developed—targeted CAs that accumulate in specific tissues and organs and allow for an improved diagnosis of these body regions,[41,42,79,82,83] as well as activatable CAs whose relaxivity reports about a specific parameter of the microenvironment in which they distribute and allow for MRI to indicate biological processes.[10,27,35,36,41,49,64,67,68,75] Most, though not all, activatable CAs reported are typically small molecular Gd chelates. The principle behind the design of such CAs is that the access of water molecules to the first coordination sphere of the chelated gadolinium ion is controllable through intramolecular rearrangement of the CA, leading to a change in relaxivity. The

percent change in relaxivity before and after stimulation is the most important factor in evaluating the efficiency of an activatable MRI CA. Among various factors influencing the relaxivity of a CA, $q$, $\tau_m$, and $\tau_R$ contribute the most to the relaxivity of an activatable CA.[41] Increasing the number of protons coordinated to the paramagnetic ions ($q$), increasing size, and increasing exchange rate are all known to increase relaxivity.[15] Herein, we briefly introduce recent advances in activatable MRI CAs sensitive to common variables in biological microenvironment, i.e., pH, bioluminescence, metal ions, redox, and enzymes.

## pH-RESPONSIVE MRI CAs

Decreased extracellular pH has been observed in cancer and various ischemic diseases and could be a biomarker for early detection or to monitor treatment efficacy.[61] Thus, the ability to non-invasively and reliably assess tissue pH is of great interest to scientists and clinicians. One of the earliest and most extensively characterized pH-sensitive MRI CAs, Gd-DOTA-4AmP$^{5-}$, was developed by Sherry and coworkers.[90] The agent, depicted in Fig. 3, consists of $Gd^{3+}$ chelated by an amido-phosphonate appended derivative of DOTA (1,4,7,10-tetraazacyclododecane-1,4,7,10-tetraacetic acid). pH sensing for this agent involves an altered proton exchange mechanism due to protonation of the phosphonate appendages that presents a 1.5-fold increase in $r_1$ over the pH range 9.5–6. The four phosphonate groups have p$K_a$s in the range 6.5–8 that, upon protonation, provide hydrogen-bond donors to the $Gd^{3+}$ bound water molecule allowing catalytic exchange of inner-sphere bound water protons with those of bulk water. A drawback of this system for pH mapping is that the tissue concentration of CA must be known for quantitation.

In response to this obstacle, Gillies and colleagues applied the Gd-DOTA-4AmP$^{5-}$ and a similar, yet pH-insensitive $Gd^{3+}$-based agent, Gd-DOTP$^{5-}$ (Fig. 3), sequentially (approx 1 h apart), to a rat tumor model.[33] With the assumption that the similar CAs had comparable biodistribution and pharmacokinetics, the researchers inferred the concentration of Gd-DOTA-4Amp$^{5-}$ based on the observed concentration of Gd-DOTP$^{5-}$. The image intensity differences between the agents at maximum enhancement were used to successfully map extracellular tissue pH in the rat glioma model. Another solution for the quantitation dilemma was recently reported by Caravan and coworkers.[32] Rather than injecting two CAs, the Gd-DOTA-4AmP$^{5-}$ was modified to incorporate a fluorine radiotracer that allows quantitation via positron emission tomography (PET) imaging. The fluorine modified CA (Fig. 3) retained its pH-responsive relaxivity measuring between 3.9 $mM^{-1}$ $s^{-1}$ at pH 6.0 and 7.4 $mM^{-1}$ $s^{-1}$ at pH 8.5. Dual-modality imaging of this activatable agent permits simultaneous quantification of the CAs tissue concentration and relaxivity thus providing a region's pH based on the linear pH-$r_1$ relationship.

Aime and coworkers investigated a responsive Gd agent that measures pH in a concentration-independent fashion through $r_2/r_1$ ratiometric analysis.[3] The Gd-DOTA functionalized polypeptide (poly-L-ornithine), shown in Fig. 4a, assembles randomly at low pH or into an ordered helix at higher pH; this pH-dependent change in conformation affects the rotational mobility of the complex yielding variation in the $r_2/r_1$ ratio. Similarly, Sherry and colleagues reported an MRI CA that utilizes altered molecular tumbling and proton exchange kinetics to magnify pH sensitivity.[4] The relaxivity and responsiveness of the previously discussed, small-molecule agent, Gd-DOTA-4AmP$^{5-}$, was improved upon through conjugation to the surface of a PAMAM dendrimer (Fig. 4b) thus producing a macromolecular sensor with ~96 pH-responsive Gd chelates. This approach affecting both molecular tumbling and exchange kinetics of inner- and outer-sphere water molecules provided

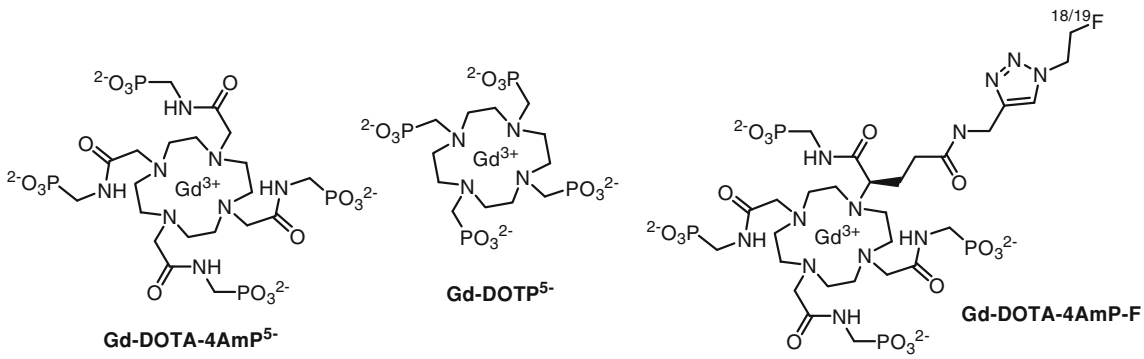


**FIGURE 3. Structure of MRI CAs: Gd-DOTA-4AmP, Gd-DOTP, and dual-modality PET/MRI CA: Gd-DOTA-4Amp-F.**

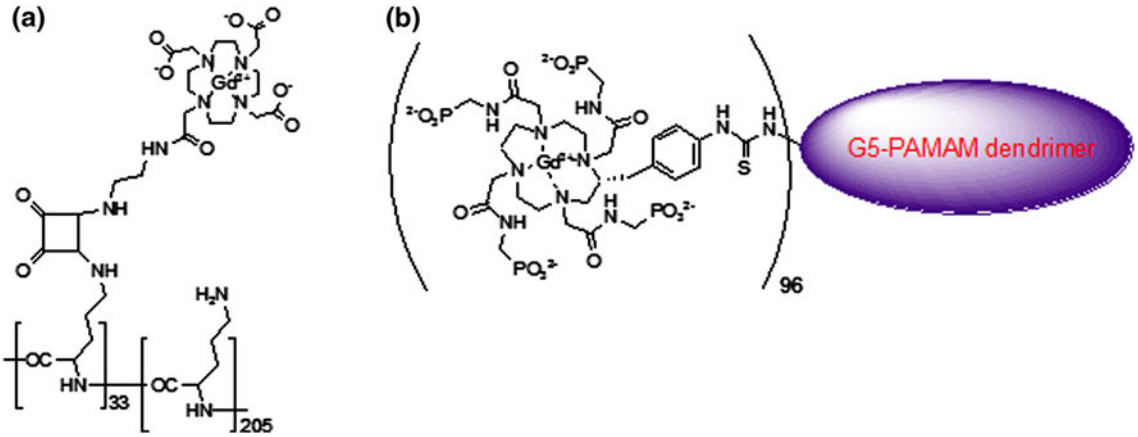


**FIGURE 4. Structures of the macromolecular, pH-sensitive CAs (a) $(Gd\text{-}DOTAam)_{33}\text{-}Orn_{205}$ and (b) Gd-DOTA-4AmP-PAMAM dendrimer. Graphic (a) modified from Chart 1 in Aime *et al.*[3] Graphic (b) modified from Ali *et al.*[4].**

increased overall relaxivity by a factor of nearly 5 and enhanced pH responsiveness for the dendrimer by means of a greater amplitude change in $r_1$ (a 2.2-fold increase was observed over the pH range 9.5–6) over the measured pH range. While the large size and ~140 kDa molecular weight of the agent positively affected its pH response, they may prove detrimental to its effectiveness *in vivo*. Dendrimers have the potential for toxicity due to slow clearance through the liver, and they may not diffuse from the vasculature as easily as small molecule CAs. Further experiments are needed to assess pharmacokinetics and biodistribution of the dendrimer based CA.

Two unconventional, Gd-based pH-responsive CAs were reported by Wilson, Toth, and coworkers in the form of gadofullerenes[76] and gadonanotubes.[37] The water-soluble gadofullerenes, $Gd@C_{60}[C(COOH)_2]_{10}$ and $Gd@C_{60}(OH)_x$, were shown to exhibit a pH-dependent reversible aggregation that results in variation of the rotational correlation time and thus variable relaxivity. As pH was decreased, the researchers observed aggregation of the agent by dynamic light scattering (DLS) size measurement. Correspondingly, the proton relaxivities of $Gd@C_{60}[C(COOH)_2]_{10}$ and $Gd@C_{60}(OH)_x$ increase by a factor of 3.8 and 2.6, respectively, with decreasing pH over the range 12–2. These gadofullerenes offer two distinct advantages towards translating them into clinically viable MRI CAs for pH sensing. First, water-soluble fullerenes have shown the ability to cross cell membranes, and second, the entrapment of $Gd^{3+}$ within the fullerene cage prevents the toxicity observed from free, unchelated $Gd^{3+}$ ion. Gadonanotubes, represented in Fig. 5, are 20–80 nm segments of single-walled carbon nanotubes that have sidewall defects in which 3–10 $Gd^{3+}$ ions cluster. The short nanotubes were prepared by a chemical cutting process that creates defects in which $Gd^{3+}$

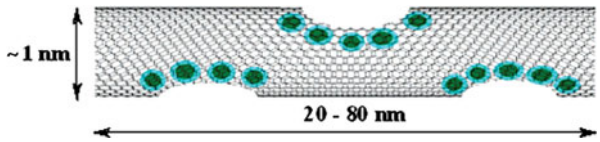


**FIGURE 5. Pictorial representation of $Gd^{3+}$ ions ( ) within the sidewall defects of a nanotube. Gd clusters measure roughly 1 × 5 nm with 3–10 $Gd^{3+}$ ions per cluster. Graphic from Fig. 1 in Hartman *et al.*[37].**

ions are loaded with chloride as counter ions. The gadonanotubes display remarkably high relaxivity (180 $mM^{-1}$ $s^{-1}$ at 1.5 T) compared to current clinically used MRI CAs. In addition, the authors report a > 3-fold increase in relaxivity observed from pH 8.3 to 6.7. While the mechanism of the pH-dependent contrast enhancement is unclear, experiments verified that $Gd^{3+}$ ion are not leaked from the nanotube clusters upon pH cycling or physiological challenges such as phosphate buffer solution (PBS), bovine serum, or heat. These results show potential for development of gadonanotubes as efficient, ultra-sensitive pH-responsive MRI CAs.

## LIGHT-RESPONSIVE MRI CAs

One of the more recent and novel advances in the field of activatable MRI probes is the development of light-responsive CAs. Bioluminescence imaging has found wide use in cell and molecular biology. Scientists and clinicians are able to use luminescence from markers such as green fluorescent protein or the luciferase system as reporters of gene expression or for cell-tracking purposes.[28] While optical imaging of bioluminescence offers the benefit of high sensitivity, it suffers the drawback of limited tissue penetration depth. Therefore, a photo-responsive, reversibly

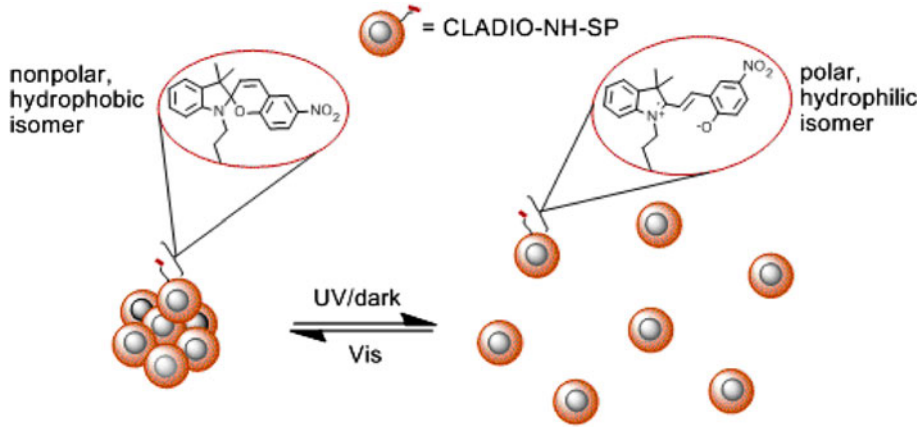


**FIGURE 6. Mechanism of reversible aggregation for light-responsive CLADIO-NH-SP. Image from Scheme 1 in Osborne *et al.*[57].**

activatable MRI CA would provide a means of imaging such bioluminescence in deep tissues. Louie and coworkers have developed a series of MRI CAs that respond to visible and UV light. Utilizing light-responsive molecular switches from the spiropyran family of compounds, they have developed both $T_1$[78,81] and $T_2$[57] CAs that can modulate MR signal with light stimulus.

The $T_1$ agents consisted of either a single nitro or dinitro-spiropyran derivative that was tethered to a DO3A chelated $Gd^{3+}$ ion. Varying degrees of light response were observed depending on the spiropyran moiety that the agent possessed. The "single nitro" version showed a 21% decrease in relaxivity (3.72–2.93 $mM^{-1}$ $s^{-1}$) in solution studies upon visible light irradiation following storage in the dark. Whereas, the dinitrospiropyran-Gd-DO3A presented an 18% decrease in relaxivity with white light stimulus (2.51–2.05 $mM^{-1}$ $s^{-1}$). Both agents exhibited reversibility with UV irradiation (at 365 nm) or storage in the dark. The observed $r_1$ modulation was attributed to a change in hydration state, $q$, of the $Gd^{3+}$ ion due to the ability of the tethered spiropyran to block water access upon absorbance of visible light. Beyond the light stimulated response, the authors note that the dinitrospiropyran-GdDO3A agent also possessed a novel NADH response that is discussed further in "Redox potential responsive MRI CAs" section of this review.

Most recently, the Louie group reported an activatable MRI $T_2$ agent, CLADIO-NH-SP, that modifies relaxation time through reversible aggregation of magnetic nanoparticles (Fig. 6).[57] This probe employs a spiropyran derivative that is covalently bound to the surface of cross-linked and aminated dextran sulfate coated iron oxide nanoparticles. The spiropyran derivative changes conformation reversibly between hydrophobic and hydrophilic isomers with UV and visible light irradiation; this conformation switching directs the aggregation and dispersion of the nanoparticles, thus regulating $T_2$ relaxation time. The authors observed nanoparticle aggregation by DLS size measurement and a 34% decrease in $T_2$ relaxation time upon visible light irradiation. In addition, the reported absorbance maximum of the spiropyran terminated CA is 563 nm which provides overlap with the emission of firefly luciferin; therefore, this light-responsive MRI probe shows promise for development as a non-invasive reporter of gene expression.

## METAL ION-RESPONSIVE MRI CAs

Metal ions play significant roles in biological signaling events, redox homeostasis, and metabolism. Therefore, it is not surprising to see research effort in the last decade towards development of activatable MRI agents responsive to biologically relevant metal ions such as $Ca^{2+}$, $Zn^{2+}$, $Fe^{2+}$, and $Cu^{+/2+}$ ions. Meade and colleagues reported the first $Ca^{2+}$-responsive MRI CA consisting of two Gd-DO3A chelates connected by a modified BAPTA (1,2-bis(*o*-aminophenoxyl)-ethane-*N*,*N*,*N*′,*N*′-tetreaacetic acid) linker (Fig. 7).[45] In the absence of $Ca^{2+}$, the carboxylate arms of the BAPTA moiety bind the chelated $Gd^{3+}$ yielding a relaxivity of 3.26 $mM^{-1}$ $s^{-1}$. In the presence of $Ca^{2+}$, the BAPTA selectively binds $Ca^{2+}$ and frees up $Gd^{3+}$ binding sites for bulk water, resulting in a relaxivity increase to 5.76 $mM^{-1}$ $s^{-1}$. The agent's BAPTA linker possesses a preference for $Ca^{2+}$ over $Mg^{2+}$ with a binding affinity in the low micromolar range which makes this CA capable of detecting intracellular $Ca^{2+}$. Since the Meade group contribution, several other lower affinity $Ca^{2+}$-sensitive CAs have been reported that utilize dual Gd-DO3A chelates with varying linkers such as BAPTA bisamide,[29] EDTA,[53] DTPA,[53] and EGTA.[5] With millimolar

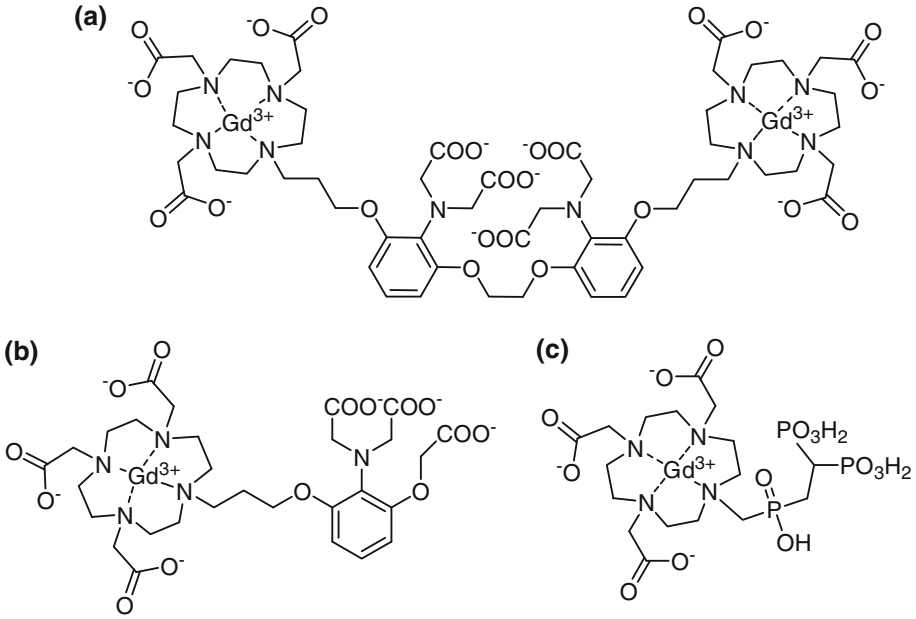


**FIGURE 7. $Ca^{2+}$-sensitive MRI CAs: (a) BAPTA linked dual Gd-DO3A; (b) Gd-DOPTRA; and (c) Gd–do3ap$^{BP}$.**

binding affinities, these agents show promise as extracellular $Ca^{2+}$ sensors.

Dhingra, Logothetis, and coworkers report an MRI CA, Gd-DOPTRA (Fig. 7), which provides nearly 100% contrast enhancement upon coordination of $Ca^{2+}$ (3.5 $mM^{-1}$ $s^{-1}$ in the absence of $Ca^{2+}$ and 6.9 $mM^{-1}$ $s^{-1}$ with addition of $Ca^{2+}$).[29] Gd-DOPTRA is composed of a Gd-DO3A unit linked to a micromolar affinity $Ca^{2+}$ chelator, APTRA (*o*-aminophenol-*N*,*N*,*O*-triacetate). This agent offers the benefits of micromolar $Ca^{2+}$ binding in a more condensed structure than those previously developed; however, specificity for $Ca^{2+}$ is to some extent compromised as this agent produces relaxivity changes in response to $Mg^{2+}$ and $Zn^{2+}$, as well. Kubicek *et al.* recently reported another activatable CA, Gd-do3ap$^{BP}$, constructed of a single Gd-DO3A core with a bisphosphonate arm (Fig. 7).[44] The bisphosphonate group coordinates the divalent metal ions $Ca^{2+}$, $Mg^{2+}$, and $Zn^{2+}$ in an apparent coordination oligomer resulting in increases in $r_1$ up to 200–500%. This staggering relaxivity enhancement is observed upon addition of 3 equiv. of metal ions to a 2 mM CA solution in a pH-dependent fashion that varies with the metal species. The authors note that the $Zn^{2+}$ concentration used is not in the biologically relevant range ($<0.1$ mM), though $Ca^{2+}$ and $Mg^{2+}$ sensing is feasible though specificity is not yet ideal.

Beyond the $T_1$ Gd-based probes, Jasanoff and coworkers report calmodulin (CaM) modified superparamagnetic iron oxide (SPIO) nanoparticles as $Ca^{2+}$-responsive MRI $T_2$ agents.[6] CaM, a calcium signaling protein, binds target peptides in response to $Ca^{2+}$ levels. By applying CaM- and peptide-conjugated SPIOs (20–100 nm) in a 3:1 ratio, the researchers observed significant changes in $T_2$ relaxivity through aggregation of the SPIOs resulting from $Ca^{2+}$ induced cross-linking of CaM and target peptides. This CA was found to detect micromolar $Ca^{2+}$ concentration in an appropriate range for intracellular $Ca^{2+}$ sensing. Furthermore, the sensitivity can be manipulated by structurally modifying the CaM or target peptides. Currently, the most significant hurdle to biological application of the existing agent is the inability to cross cellular membranes. Further surface modification is required to address this issue.

Similar to those of $Ca^{2+}$, Gd-DO3A based agents selectively responsive to $Zn^{2+}$ have also been developed. The Meade group produced two MRI CAs with $>100\%$ increases in relaxivity upon $Zn^{2+}$ detection. Gd-daa3[50] and Gd-apa3[48] provide selective $Zn^{2+}$ binding over other biologically abundant cations such as $Ca^{2+}$, $Mg^{2+}$, $Na^+$, and $K^+$. Recently, the $Zn^{2+}$-responsive CA, Gd-DOTA-diBPEN, has been found to increase in relaxivity 165% (6.6–17.4 $mM^{-1}$ $s^{-1}$) due to an interaction with human serum albumin (HSA).[31] In the absence of HSA, the relaxivity increase is a modest 20% upon $Zn^{2+}$ detection, suggesting $\tau_R$ modulation. Gd-DOTA-diBPEN does not respond to $Ca^{2+}$ or $Mg^{2+}$, yet can detect $Zn^{2+}$ down to 30 $\mu$M in the presence of HSA as observed in *in vitro* imaging studies.

Though iron-sensing CAs have not been characterized in literature, several Gd chelates that also coordinate Fe with corresponding relaxivity increases have

been reported.[1,24,58,59] For instance, Parac-Vogt *et al.* describe an MRI probe, Gd-DTPA-phen, that self-assembles 3:1 with an $Fe^{2+}$ ion.[58] The supramolecular complex, $[(\text{Gd-DTPA-phen})_3\text{Fe}]^-$, has a relaxivity of 9.5 $mM^{-1}$ $s^{-1}$ as compared to 3.9 $mM^{-1}$ $s^{-1}$ for Gd-DTPA. Similarly, Desreux and coworkers reported a 77% increase in relaxivity upon coordination of $Fe^{2+}$ with three GdPhenHDO3A complexes.[59] Neither of these cases address the sensitivity or specificity for $Fe^{2+}$ over other metal ions so further exploration into their suitability as Fe-sensitive CAs is needed.

Cu-sensing agents are among the newest metal ion-responsive MRI CAs. Chang and coworkers recently reported a series of sensors that utilize a Gd-DO3A core with a Cu ion binding thioether pendant arm (Fig. 8).[65] These agents provide $r_1$ modulation through altered hydration state of the $Gd^{3+}$ ion. In the absence of copper, the pendant arm appears to block water access to the Gd core yielding $q = 0.3$; upon addition of 1 equiv. $Cu^+$, $q$ increases to 2. The most responsive of these agents yields a 360% increase in relaxivity upon $Cu^+$ binding (1.5–6.9 $mM^{-1}$ $s^{-1}$ with $Cu^+$). In addition, the Chang group has developed a sensor that can detect $Cu^{2+}$ with high affinity through inclusion of an O donor in the pendant arm (Fig. 8c).[65] These CAs offer significant benefits over those previously reported for $Cu^{2+}$ detection in that they possess picomolar range $Cu^+/Cu^{2+}$ binding affinity with high specificity over other biologically endogenous metal ions. In the realm of responsive $T_2$ agents, Patel *et al.* reported SPIO nanoparticles surface-modified with DOTA for the chelation of $Cu^{2+}$.[60] These agents were developed as dual-modality PET/MRI CAs, but a strong increase in $r_2$ relaxivity (~300%) upon coordination of $Cu^{2+}$ ions points to potential use as activatable MRI CAs responsive to micromolar $Cu^{2+}$ concentration. The authors speculate as to the mechanism causing $r_2$ increase, but indicate that aggregation of the nanoparticles is not observed. The association of water molecules at the DOTA bound $Cu^{2+}$ ion may facilitate transmission of the magnetic induction of the SPIO to bulk water, or the surface modification could possibly shorten the residence lifetime of coordinated water.

## REDOX POTENTIAL-RESPONSIVE MRI CAs

Redox reactions are widely seen in biochemical activities. Disruption of redox homoeostasis may lead to many pathological conditions, such as atherosclerosis, stroke, Alzheimer's disease, Parkinson's disease, and cancer, etc.[39] However, non-invasive observation of intracellular redox activities and their relationship to physiological function is still a challenge for molecular imaging, most likely due to the lack of appropriate probes responsive to redox potential.[14,40,51]

Louie and co-workers have developed activatable MRI CAs sensitive to reduced nicotinamide adenine dinucleotide (NADH), the principal electron donor for the respiratory chain in mammalian cells.[43,80,81] In the first generation agent a spirobenzopyran molecule, which is responsive to changes in light and electrical activities,[7,63,91] was coupled to Gd-DO3A (DO3A: 1,4,7,10-tetraazacyclododecane-1,4,7-trisacetic acid). As described earlier in the paper, when photo-stimulation was applied, the structural change of the spirobenzopyran moiety in the resultant agent caused the two isomers to have different contrast enhancement properties for MRI. However, the CA was not responsive to electrical activity or redox potential.[78] By adding a strong electron-withdrawing nitro group to the indole ring, the $r_1$ relaxivity of the resultant dinitrospiropyran-Gd-DO3A is found to be responsive to both light and NADH. When in the dark, the CA is in its open (MC) form and has an $r_1$ relaxivity of 2.51 $mM^{-1}$ $s^{-1}$. After irradiation with visible light or mixing with NADH, the CA experiences a color change and its $r_1$ relaxivity decreases to 2.05 and 1.86 $mM^{-1}$ $s^{-1}$, respectively.[81] The second generation agent employs spironaphthoxazines instead of

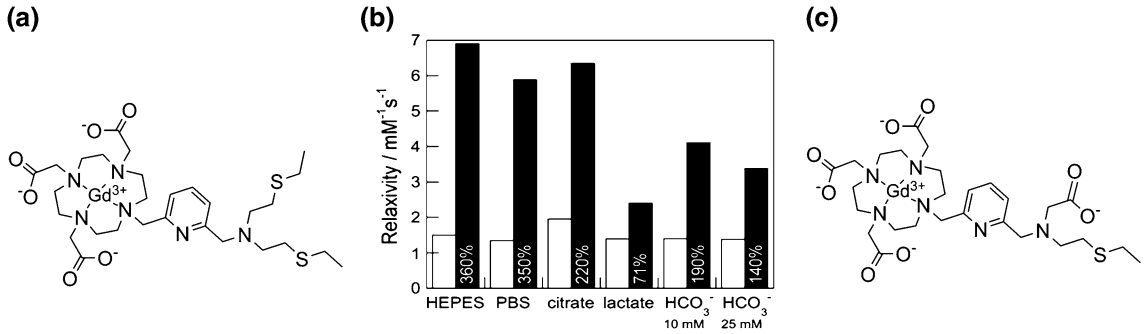


**FIGURE 8. Gd-DO3A-based MRI CA. (a) with a $Cu^+$-binding thioether pendant arm demonstrating; (b) $r_1$ relaxivity increases (with corresponding percent increase given) to 1 equiv. of $Cu^+$ in the presence of various biological anions. White bars represent CA relaxivities in the absence of $Cu^+$ while the black bars represent relaxivities with addition of $Cu^+$ (60 MHz, 37 °C, pH = 7.4); (c) shows the $Cu^{2+}$ activated CA. Graph from Fig. 7 in Que *et al.*[65].**

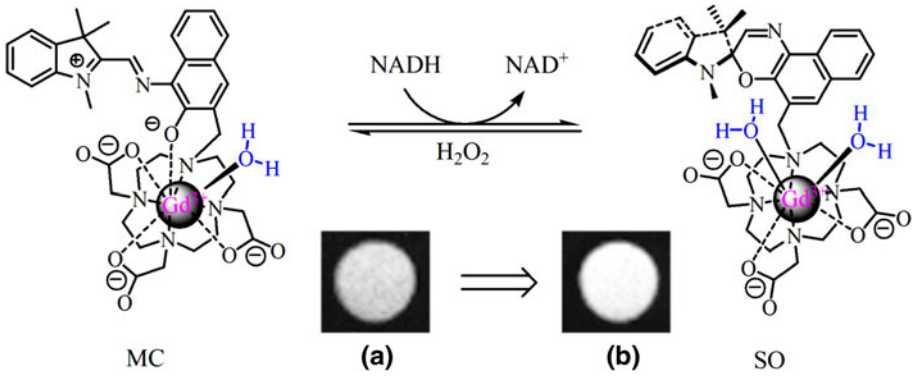


**FIGURE 9. The structural and hydration number ($q$) changes in the first coordination sphere of Gd(III) of spirooxazine-Gd-DO3A triggered by NADH and hydrogen peroxide. $T_1$-weighted MRI images of (a) spirooxazine-Gd-DO3A and (b) the mixture of spirooxazine-Gd-DO3A and NADH (Gd:NADH = 1:1), in P388D1 murine macrophages. Images modified from Scheme 2 and Fig. 5 in Tu *et al.*[80].**

spirobenzopyran.[23,89] In the dark the agent has an $r_1$ relaxivity of 5.58 $mM^{-1}$ $s^{-1}$ and an average of 1.26 water molecules coordinated with the Gd(III). In the presence of NADH, as shown in Fig. 11, the agent undergoes an isomerization and its hydration number ($q$) increased to 2.01, which leads to an $r_1$ relaxivity increase of 54%. The $T_1$ value can be fully restored after applying hydrogen peroxide to the system. Macrophages are incubated with spirooxazine-Gd-DO3A, then exposed to externally applied NADH. Cells exposed to NADH show substantial contrast enhancement, as shown in Figs. 9a and 9b.

Unlike the Gd agents described above whose redox reactions take place on the ligand, redox reactions of activatable iron (Fe) agent occur directly at the metal center. Jasanoff and coworkers report injection of iron-containing hemoglobin (Hb) into blowflies; they found that the Hb can permeate through relatively dense neural tissue without obvious disruption to physiology and the oxidation state of Hb is dependent on the partial pressure of oxygen, $pO_2$. Oxygen is an important parameter in living systems. Variations in $pO_2$ have been relevant to many diseases, such as stroke and tumors.[52,62] Hb-injected flies show approximate 40–50% changes in signal intensity when external $O_2$ levels are manipulated artificially from 0 to 21%, because the iron in the porphyrin ring of Hb changes in redox state from diamagnetic Fe(II) to paramagnetic Fe(III) in the presence of $O_2$. *In vivo* $T_2$-weighted MRI shows that a small amount of Hb is able to produce substantial $pO_2$-dependent signal contrast, and the contrast changes can be roughly calibrated if necessary.[74]

## ENZYME-RESPONSIVE MRI CAs

The enzymatically modulated MRI CAs could provide an effective means of measuring enzyme activity, detecting enzyme location, and assaying gene expression. Meade and coworkers developed the first example of enzyme-sensitive MRI CA and demonstrated the principle of enzymatic activation of an MRI CA by beta-galactosidase.[47,54] More recently, Meade group developed a Gd-DO3A derivative which shows relaxivity change in the presence of $\beta$-glucuronidase.[30] As shown in Fig. 10, the agent bears a pendant $\beta$-glucuronic acid moiety, the substrate of $\beta$-glucuronidase, on an arm of DO3A. In the presence of bovine liver $\beta$-glucuronidase, an ether bond of the agent was enzymatically cleaved, resulting in a self-immolating reaction passing through the spacer until the breakage of the amide bond (red arrow), and restricting water access to the paramagnetic ion. In comparison with the original beta-galactosidase agent, the resultant 2-aminoethyl-Gd-DO3A has an extra amine group (blue arrow) coordinated to the metal center, thus is expected to have a lower $q$ number and relaxivity value. However, the relaxivity changes of the enzymatic hydrolytic reaction markedly depended on buffer composition employed: the relaxivity increased in a buffer mimicking *in vivo* anion concentrations by 17%, while the relaxivity decreased by 27% for the same experiment in human blood serum.

Besides hydrolases, oxidoreductases also have been targets in the exploration of enzyme-sensitive paramagnetic CAs. A MR signal amplification strategy has been developed based on oxidoreductase-mediated polymerization of paramagnetic Gd substrates into oligomers of higher magnetic relaxivity.[8,9,11,18–21,55,66,67,69–72] Benzene-1,2-diol which is known to be a substrate of oxidized peroxidases was linked to a Gd-DOTA chelate, and the resultant agent acted as a monomer (Fig. 11a). In the presence of peroxidase, the monomers were induced to form radicals that trigger the rapid condensation into paramagnetic oligomers leading to a threefold increase in $r_1$

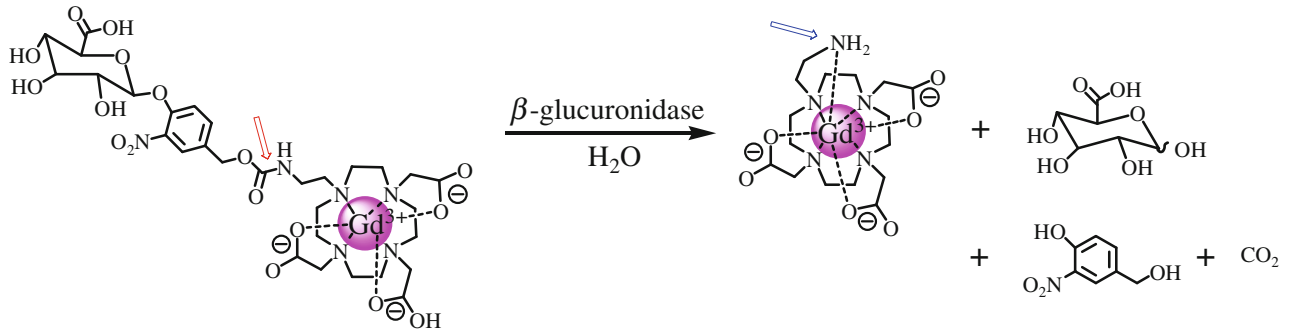


**FIGURE 10. Schematic illustration of β-glucuronidase-catalyzed cleavage of a Gd-DO3A type chelate bearing the substrate of β-glucuronidase.**

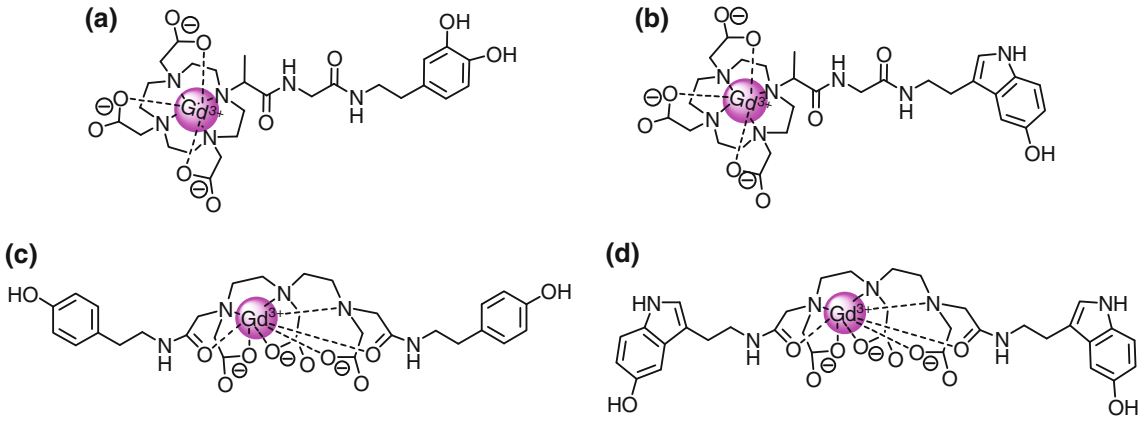


**FIGURE 11. Schematic illustration of Gd chelates sensitive to myeloperoxidase (MPO).**

relaxivity due to an increase in $\tau_R$. By this signal amplification mechanism, horseradish peroxidase (HRP) could be detected in the nanomolar range. *In vivo* MRI was also performed to detect E-selectin expression on human endothelial cells in culture by using a highly specific first antibody, followed by a secondary antibody conjugate with HRP.[8]

By substituting the catechol moiety with a serotonin moiety (Fig. 11b), the Gd(III) chelate was oriented to be responsive to myeloperoxidase (MPO), a key-marker of inflammation processes involved in numerous pathologies. Serotonin is a naturally occurring neurotransmitter that functions as a reducing substrate for MPO. The agent is efficiently polymerized in the presence of human neutrophil MPO resulting in a 70–100% increase in proton relaxivity.[20] The MPO-enhanced MRI signal was also obtained when using Gd-DTPA bearing either tyramide (Fig. 11c or 5-hydroxytryptamide-(serotonin) (Fig. 11d) groups.[70] The activation involves the formation of a radical species that can proceed differently depending on the considered complex. Two mechanisms have been suggested.[71] One is related to the oligomerization of the complex and the other is related to the formation of cross-linked structures with proteins, as shown in Fig. 12. However, it is also found that sometimes the Gd agent may utilize both mechanisms when activated.[71]

The Gd-DTPA-serotonin, referred as MPO-Gd, was further applied for *in vivo* MRI of ischemic injury of the myocardium which causes timed recruitment of neutrophils and monocytes/macrophages, which produce substantial amounts of local MPO.[55] Myocardial infarction (MI) was induced by left coronary artery ligation of normal (C57BL/6) mice.[56] After 2 days coronary ligation, mice were scanned before and up to 2 h after injection of equal doses of MPO-Gd and control Gd-DTPA. The signal enhancement was observable in the kinetic infarct at 10 and 30 min after injection of Gd-DTPA with peak enhancement at 10 min, then completely returned to the original status after 60 min. After injection of MPO-Gd, the peak enhancement appeared at 60 min and the signal intensity was significantly higher in comparison with that of Gd-DTPA. The enhancement was still observable even at 120 min after injection.[55]

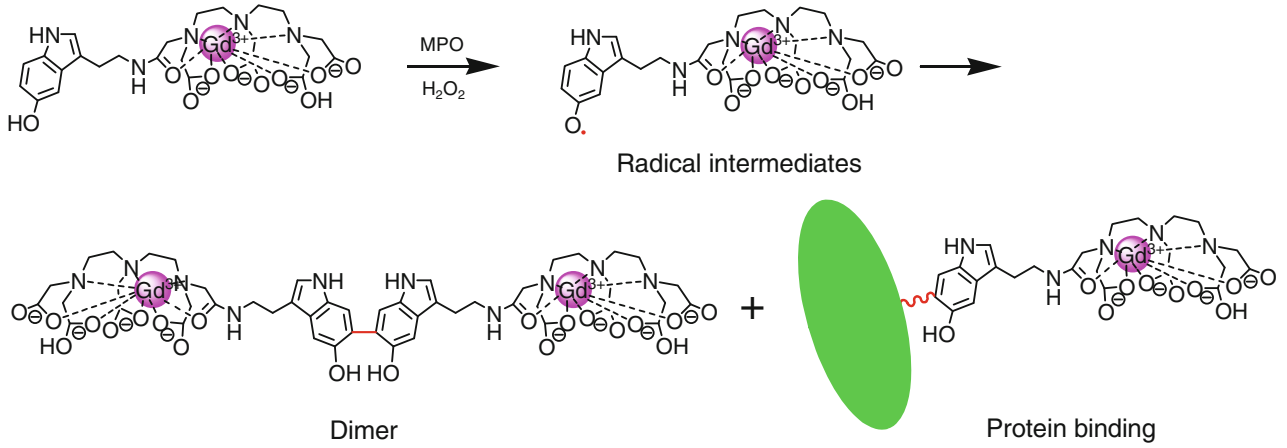


**FIGURE 12. The activation mechanism of the Gd agent by the MPO–$H_2O_2$ system. The MPO-sensitive moiety in the gadolinium complex can be oxidized by MPO in the presence of $H_2O_2$ to generate a radical intermediate. The radicals can form dimers and oligomers with other radicals, or can bind to other phenolic residues on the protein surface. Both activation effects will decrease $\tau_R$, resulting in higher $r_1$ relaxivity. Images modified from Scheme 2 in Rodriguez *et al.*[71].**

## CONCLUDING REMARKS

During the last decade, emergence of suitable CAs which report on physiological processes has expanded the scope of MRI beyond anatomical and functional imaging to also convey information at the cellular or even molecular level. Though a variety of publications have shown the great potential of activatable CAs to report about changes of diagnostically relevant variables of physicochemical microenvironments *in vitro*, so far only very few examples have moved into *in vivo* studies. An active and effective collaboration between chemists, biologists, and clinicians is particularly critical in bringing activatable CAs with outstanding properties into realistic uses. Feedback from biologists, imagers, and clinicians will be crucial for chemists to design more versatile and controllably activatable CAs whose structures can be readily and finely tuned to undergo either intramolecular transitions or intermolecular interactions resulting in greater relaxivity changes in response to variables of physiological microenvironments.

## ACKNOWLEDGMENTS

The authors wish to acknowledge the National Institute of Health (HL081108-01, EB008576-01, and EB006192) and the NMR award of the University of California, Davis for support of this work.

## OPEN ACCESS



## REFERENCES

[1]Aime, S., M. Botta, M. Fasano, and E. Terreno. Paramagnetic gd-iii-fe-iii heterobimetallic complexes of dtpa-bis-salicylamide. *Spectrochim. Acta A Mol. Biomol. Spectrosc.* 49:1315–1322, 1993.

[2]Aime, S., and P. Caravan. Biodistribution of gadolinium-based contrast agents, including gadolinium deposition. *J. Magn. Reson. Imaging* 30:1259–1267, 2009.

[3]Aime, S., F. Fedeli, A. Sanino, and E. Terreno. A r2/r1 ratiometric procedure for a concentration-independent, pH-responsive, Gd(III)-based MRI agent. *J. Am. Chem. Soc.* 128:11326–11327, 2006.

[4]Ali, M. M., M. Woods, P. Caravan, A. C. L. Opina, M. Spiller, J. C. Fettinger, and A. D. Sherry. Synthesis and relaxometric studies of a dendrimer-based pH-responsive MRI contrast agent. *Chem. Eur. J.* 14:7250–7258, 2008.

[5]Angelovski, G., P. Fouskova, I. Mamedov, S. Canals, E. Toth, and N. K. Logothetis. Smart magnetic resonance imaging agents that sense extracellular calcium fluctuations. *ChemBioChem.* 9:1729–1734, 2008.

[6]Atanasijevic, T., M. Shusteff, P. Fam, and A. Jasanoff. Calcium-sensitive MRI contrast agents based on superparamagnetic iron oxide nanoparticles and calmodulin. *Proc. Natl. Acad. Sci. USA* 103:14707–14712, 2006.

[7]Berkovic, G., V. Krongauz, and V. Weiss. Spiropyrans and spirooxazines for memories and switches. *Chem. Rev.* 100:1741–1753, 2000.

[8]Bogdanov, Jr., A., L. Matuszewski, C. Bremer, A. Petrovsky, and R. Weissleder. Oligomerization of paramagnetic substrates result in signal amplification and can be used for mr imaging of molecular targets. *Mol. Imaging* 1:16–23, 2002.

[9]Bogdanov, A. A., M. Querol, and J. W. Chen. Visualization of the enzymatic activity in living systems using activated nmr contrast agents. *Biofizika* 52:389–400, 2007.

[10]Bonnet, C. S., and E. Toth. Smart MR imaging agents relevant to potential neurologic applications. *Am. J. Neuroradiol.* 31:401–409, 2010.
[11]Breckwoldt, M. O., J. W. Chen, L. Stangenberg, E. Aikawa, E. Rodriguez, S. M. Qiu, M. A. Moskowitz, and R. Weissleder. Tracking the inflammatory response in stroke in vivo by sensing the enzyme myeloperoxidase. *Proc. Nat. Acad. Sci. USA* 105:18584–18589, 2008.
[12]Britton, M. M. Magnetic resonance imaging of chemistry. *Chem. Soc. Rev.* 39:4036–4043, 2010.
[13]Brown, M. A., and R. C. Semelka. MRI: Basic Principles and Applications. Hoboken, NJ: Wiley-Blackwell/John Wiley & Sons, 2010.
[14]Cao, Q. Z., W. B. Cai, G. Niu, L. N. He, and X. Y. Chen. Multimodality imaging of il-18-binding protein-fc therapy of experimental lung metastasis. *Clin. Cancer Res.* 14:6137–6145, 2008.
[15]Caravan, P. Strategies for increasing the sensitivity of gadolinium based MRI contrast agents. *Chem. Soc. Rev.* 35:512–523, 2006.
[16]Caravan, P., J. J. Ellison, T. J. McMurry, and R. B. Lauffer. Gadolinium(III) chelates as MRI contrast agents: structure, dynamics, and applications. *Chem. Rev.* 99:2293–2352, 1999.
[17]Chan, K. W. Y., and W. T. Wong. Small molecular gadolinium(III) complexes as MRI contrast agents for diagnostic imaging. *Coord. Chem. Rev.* 251:2428–2451, 2007.
[18]Chang, Y. T., C. M. Cheng, Y. Z. Su, W. T. Lee, J. S. Hsu, G. C. Liu, T. L. Cheng, and Y. M. Wang. Synthesis and characterization of a new bioactivated paramagnetic gadolinium(III) complex Gd(DOTA-fpg)($H_2O$) for tracing gene expression. *Bioconjugate Chem.* 18:1716–1727, 2007.
[19]Chen, J. W., M. O. Breckwoldt, E. Aikawa, G. Chiang, and R. Weissleder. Myeloperoxidase-targeted imaging of active inflammatory lesions in murine experimental autoimmune encephalomyelitis. *Brain* 131:1123–1133, 2008.
[20]Chen, J. W., W. Pham, R. Weissleder, and A. Bogdanov. Human myeloperoxidase: a potential target for molecular mr imaging in atherosclerosis. *Magn. Reson. Med.* 52:1021–1028, 2004.
[21]Chen, J. W., M. Q. Sans, A. Bogdanov, and R. Weissleder. Imaging of myeloperoxidase in mice by using novel amplifiable paramagnetic substrates. *Radiology* 240:473–481, 2006.
[22]Cherry, S. R., A. Y. Louie, and R. E. Jacobs. The integration of positron emission tomography with magnetic resonance imaging. *Proc. IEEE* 96:416–438, 2008.
[23]Chu, N. Y. C. Photochromism of spiroindolinonaphthoxazine.1. Photophysical properties. *Can. J. Chem.* 61:300–305, 1983.
[24]Comblin, V., D. Gilsoul, M. Hermann, V. Humblet, V. Jacques, M. Mesbahi, C. Sauvage, and J. F. Desreux. Designing new mri contrast agents: a coordination chemistry challenge. *Coord. Chem. Rev* 185–186:451–470, 1999.
[25]Cormode, D. P., T. Skajaa, Z. A. Fayad, and W. J. M. Mulder. Nanotechnology in medical imaging probe design and applications. *Arterioscler. Thromb. Vasc. Biol.* 29:992–1000, 2009.
[26]Datta, A., and K. N. Raymond. Gd-hydroxypyridinone (hopo)-based high-relaxivity magnetic resonance imaging (MRI) contrast agents. *Acc. Chem. Res.* 42:938–947, 2009.
[27]De Leon-Rodriguez, L. M., A. J. M. Lubag, C. R. Malloy, G. V. Martinez, R. J. Gillies, and A. D. Sherry. Responsive MRI agents for sensing metabolism in vivo. *Acc. Chem. Res.* 42:948–957, 2009.
[28]de Wet, J. R., K. V. Wood, M. DeLuca, D. R. Helinski, and S. Subramani. Firefly luciferase gene: structure and expression in mammalian cells. *Mol. Cell. Biol.* 7:725–737, 1987.
[29]Dhingra, K., P. Fousková, G. Angelovski, M. Maier, N. Logothetis, and É. Tóth. Towards extracellular $Ca^{2+}$ sensing by MRI: Synthesis and calcium-dependent $^1H$ and $^{17}O$ relaxation studies of two novel bismacrocyclic $Gd^{3+}$ complexes. *J. Biol. Inorg. Chem.* 13:35–46, 2008.
[30]Duimstra, J. A., F. J. Femia, and T. J. Meade. A gadolinium chelate for detection of beta-glucuronidase: a self-immolative approach. *J. Am. Chem. Soc.* 127:12847–12855, 2005.
[31]Esqueda, A. C., J. A. López, G. Andreu-de-Riquer, J. C. Alvarado-Monzón, J. Ratnakar, A. J. M. Lubag, A. D. Sherry, and L. M. De León-Rodríguez. A new gadolinium-based MRI zinc sensor. *J. Am. Chem. Soc.* 131:11387–11391, 2009.
[32]Frullano, L., C. Catana, T. Benner, A. D. Sherry, and P. Caravan. Bimodal MR–PET agent for quantitative ph imaging. *Angew. Chem. Int. Ed.* 49:2382–2384, 2010.
[33]Garcia-Martin, M. L., G. V. Martinez, N. Raghunand, A. Dean Sherry, S. Zhang, and R. J. Gillies. High resolution phe imaging of rat glioma using pH-dependent relaxivity. *Magn. Reson. Med.* 55:309–315, 2006.
[34]Geraldes, C. F., and S. Laurent. Classification and basic properties of contrast agents for magnetic resonance imaging. *Contrast Med. Mol. Imaging* 4:1–23, 2009.
[35]Hanaoka, K. Development of responsive lanthanide-based magnetic resonance imaging and luminescent probes for biological applications. *Chem. Pharm. Bull.* 58:1283–1294, 2010.
[36]Harney, A. S., and T. J. Meade. Molecular imaging of in vivo gene expression. *Future Med. Chem.* 2:503–519, 2010.
[37]Hartman, K. B., S. Laus, R. D. Bolskar, R. Muthupillai, L. Helm, E. Toth, A. E. Merbach, and L. J. Wilson. Gadonanotubes as ultrasensitive pH-smart probes for magnetic resonance imaging. *Nano Lett.* 8:415–419, 2008.
[38]Hermann, P., J. Kotek, V. Kubicek, and I. Lukes. Gadolinium(III) complexes as MRI contrast agents: ligand design and properties of the complexes. *Dalton Trans.* 3027–3047, 2008.
[39]Hoye, A. T., J. E. Davoren, P. Wipf, M. P. Fink, and V. E. Kagan. Targeting mitochondria. *Acc. Chem. Res.* 41:87–97, 2008.
[40]Hyodo, F., B. P. Soule, K. I. Matsumoto, S. Matusmoto, J. A. Cook, E. Hyodo, A. L. Sowers, M. C. Krishna, and J. B. Mitchell. Assessment of tissue redox status using metabolic responsive contrast agents and magnetic resonance imaging. *J. Pharm. Pharmacol.* 60:1049–1060, 2008.
[41]Jacques, V., and J. F. Desreux. Topics in Current Chemistry: Contrast Agents I, Vol. 221. Berlin: Springer-Verlag, pp. 123–164, 2002.
[42]Kamaly, N., A. D. Miller, and J. D. Bell. Chemistry of tumour targeted t-1 based MRI contrast agents. *Curr. Top. Med. Chem.* 10:1158–1183, 2010.
[43]Klaidman, L. K., A. C. Leung, and J. D. Adams. High-performance liquid-chromatography analysis of oxidized and reduced pyridine dinucleotides in specific brain-regions. *Anal. Biochem.* 228:312–317, 1995.
[44]Kubíček, V., T. Vitha, J. Kotek, P. Hermann, L. V. Elst, R. N. Muller, I. Lukeš, and J. A. Peters. Towards MRI contrast agents responsive to Ca(II) and Mg(II) ions: metal-induced oligomerization of DOTA–bisphosphonate conjugates. *Contrast Med. Mol. Imaging* 5:294–296, 2010.

[45]Li, W.-H., S. E. Fraser, and T. J. Meade. A calcium-sensitive magnetic resonance imaging contrast agent. *J. Am. Chem. Soc*. 121:1413–1414, 1999.
[46]Louie, A. Multimodality imaging probes: design and challenges. *Chem. Rev*. 110:3146–3195, 2010.
[47]Louie, A. Y., M. M. Huber, E. T. Ahrens, U. Rothbacher, R. Moats, R. E. Jacobs, S. E. Fraser, and T. J. Meade. In vivo visualization of gene expression using magnetic resonance imaging. *Nat. Biotechnol*. 18:321–325, 2000.
[48]Major, J. L., R. M. Boiteau, and T. J. Meade. Mechanisms of ZnII-activated magnetic resonance imaging agents. *Inorg. Chem*. 47:10788–10795, 2008.
[49]Major, J. L., and T. J. Meade. Bioresponsive, cell-penetrating, and multimeric MR contrast agents. *Acc. Chem. Res*. 42:893–903, 2009.
[50]Major, J. L., G. Parigi, C. Luchinat, and T. J. Meade. The synthesis and in vitro testing of a zinc-activated MRI contrast agent. *Proc. Natl. Acad. Sci. USA* 104:13881–13886, 2007.
[51]Mankoff, D. A. A definition of molecular imaging. *J. Nucl. Med*. 48:18N–21N, 2007.
[52]Mason, R. P., S. Ran, and P. E. Thorpe. Quantitative assessment of tumor oxygen dynamics: molecular imaging for prognostic radiology. *J Cell Biochem* 39:45–53, 2002.
[53]Mishra, A., P. Fousková, G. Angelovski, E. Balogh, A. K. Mishra, N. K. Logothetis, and É. Tóth. Facile synthesis and relaxation properties of novel bispolyazamacrocyclic $Gd^{3+}$ complexes: an attempt towards calcium-sensitive mri contrast agents. *Inorg. Chem*. 47:1370–1381, 2008.
[54]Moats, R. A., S. E. Fraser, and T. J. Meade. A "smart" magnetic resonance imaging agent that reports on specific enzymatic activity. *Angew. Chem. Int. Ed*. 36:726–728, 1997.
[55]Nahrendorf, M., D. Sosnovik, J. W. Chen, P. Panizzi, J. L. Figueiredo, E. Aikawa, P. Libby, F. K. Swirski, and R. Weissleder. Activatable magnetic resonance imaging agent reports myeloperoxidase activity in healing infarcts and noninvasively detects the antiinflammatory effects of atorvastatin on ischemia-reperfusion injury. *Circulation* 117:1153–1160, 2008.
[56]Nahrendorf, M., D. E. Sosnovik, P. Waterman, F. K. Swirski, A. N. Pande, E. Aikawa, J. L. Figueiredo, M. J. Pittet, and R. Weissleder. Dual channel optical tomographic imaging of leukocyte recruitment and protease activity in the healing myocardial infarct. *Circ. Res*. 100:1218–1225, 2007.
[57]Osborne, E. A., B. R. Jarrett, C. Tu, and A. Y. Louie. Modulation of T2 relaxation time by light-induced, reversible aggregation of magnetic nanoparticles. *J. Am. Chem. Soc*. 132:5934–5935, 2010.
[58]Parac-Vogt, T. N., L. V. Elst, K. Kimpe, S. Laurent, C. Burtéa, F. Chen, R. V. Deun, Y. Ni, R. N. Muller, and K. Binnemans. Pharmacokinetic and in vivo evaluation of a self-assembled gadolinium(III)-iron(II) contrast agent with high relaxivity. *Contrast Med. Mol. Imaging* 1:267–278, 2006.
[59]Paris, J., C. Gameiro, V. Humblet, P. K. Mohapatra, V. Jacques, and J. F. Desreux. Auto-assembling of ditopic macrocyclic lanthanide chelates with transition-metal ions. Rigid multimetallic high relaxivity contrast agents for magnetic resonance imaging. *Inorg. Chem*. 45:5092–5102, 2006.
[60]Patel, D., A. Kell, B. Simard, B. Xiang, H. Y. Lin, and G. Tian. The cell labeling efficacy, cytotoxicity and relaxivity of copper-activated MRI/PET imaging contrast agents. *Biomaterials* 32:1167–1176, 2011.
[61]Pérez-Mayoral, E., V. Negri, J. Soler-Padrós, S. Cerdán, and P. Ballesteros. Chemistry of paramagnetic and diamagnetic contrast agents for magnetic resonance imaging and spectroscopy: pH responsive contrast agents. *Eur. J. Radiol*. 67:453–458, 2008.
[62]Powers, W. J., R. L. Grubb, D. Darriet, and M. E. Raichle. Cerebral blood-flow and cerebral metabolic-rate of oxygen requirements for cerebral function and viability in humans. *J. Cereb. Blood Flow Metab*. 5:600–608, 1985.
[63]Preigh, M. J., M. T. Stauffer, F. T. Lin, and S. G. Weber. Anodic oxidation mechanism of a spiropyran. *J. Chem. Soc. Faraday Trans*. 92:3991–3996, 1996.
[64]Que, E. L., and C. J. Chang. Responsive magnetic resonance imaging contrast agents as chemical sensors for metals in biology and medicine. *Chem. Soc. Rev*. 39:51–60, 2010.
[65]Que, E. L., E. Gianolio, S. L. Baker, A. P. Wong, S. Aime, and C. J. Chang. Copper-responsive magnetic resonance imaging contrast agents. *J. Am. Chem. Soc*. 131:8527–8536, 2009.
[66]Querol, M., D. G. Bennett, C. Sotak, H. W. Kang, and A. Bogdanov. A paramagnetic contrast agent for detecting tyrosinase activity. *ChemBioChem*. 8:1637–1641, 2007.
[67]Querol, M., and A. Bogdanov. Amplification strategies in mr imaging: activation and accumulation of sensing contrast agents (scas). *J. Magn. Reson. Imaging* 24:971–982, 2006.
[68]Querol, M., and A. Bogdanov, Jr. Environment-sensitive and enzyme-sensitive MR contrast agents. In: Molecular imaging II. Handbook of experimental pharmacology, Vol. 185/II, edited by W. Semmler, and M. Schwaiger. Berlin: Springer-Verlag, 2008, pp. 37–57.
[69]Querol, M., J. W. Chen, and A. A. Bogdanov. A paramagnetic contrast agent with myeloperoxidase-sensing properties. *Org. Biomol. Chem*. 4:1887–1895, 2006.
[70]Querol, M., J. W. Chen, R. Weissleder, and A. Bogdanov. DTPA-bisamide-based MR sensor agents for peroxidase imaging. *Org. Lett*. 7:1719–1722, 2005.
[71]Rodriguez, E., M. Nilges, R. Weissleder, and J. W. Chen. Activatable magnetic resonance imaging agents for myeloperoxidase sensing: mechanism of activation, stability, and toxicity. *J. Am. Chem. Soc*. 132:168–177, 2010.
[72]Ronald, J. A., J. W. Chen, Y. X. Chen, A. M. Hamilton, E. Rodriguez, F. Reynolds, R. A. Hegele, K. A. Rogers, M. Querol, A. Bogdanov, R. Weissleder, and B. K. Rutt. Enzyme-sensitive magnetic resonance imaging targeting myeloperoxidase identifies active inflammation in experimental rabbit atherosclerotic plaques. *Circulation* 120:592–599, 2009.
[73]Runge, V. M. Advances in diagnostic radiology. *Invest. Radiol*. 45:823–826, 2010.
[74]Sun, P. Z., Z. B. Schoening, and A. Jasanoff. In vivo oxygen detection using exogenous hemoglobin as a contrast agent in magnetic resonance microscopy. *Magn. Reson. Med*. 49:609–614, 2003.
[75]Terreno, E., D. D. Castelli, A. Viale, and S. Aime. Challenges for molecular magnetic resonance imaging. *Chem. Rev*. 110:3019–3042, 2010.
[76]Tóth, É., R. D. Bolskar, A. Borel, G. González, L. Helm, A. E. Merbach, B. Sitharaman, and L. J. Wilson. Water-soluble gadofullerenes: toward high-relaxivity, pH-responsive MRI contrast agents. *J. Am. Chem. Soc*. 127:799–805, 2004.

[77]Toth, E., L. Helm, and A. E. Merbach. Topics in Current Chemistry: Contrast Agents I, Vol. 221. Berlin: Springer-Verlag, pp. 61–101, 2002.
[78]Tu, C. Q., and A. Y. Louie. Photochromically-controlled, reversibly-activated MRI and optical contrast agent. *Chem. Commun*. 1331–1333, 2007.
[79]Tu, C. Q., X. C. Ma, P. Pantazis, S. M. Kauzlarich, and A. Y. Louie. Paramagnetic, silicon quantum dots for magnetic resonance and two-photon imaging of macrophages. *J. Am. Chem. Soc*. 132:2016–2023, 2010.
[80]Tu, C., R. Nagao, and A. Y. Louie. Multimodal magnetic-resonance/optical-imaging contrast agent sensitive to nadh. *Angew. Chem. Int. Ed*. 48:6547–6551, 2009.
[81]Tu, C. Q., E. A. Osborne, and A. Y. Louie. Synthesis and characterization of a redox- and light-sensitive MRI contrast agent. *Tetrahedron* 65:1241–1246, 2009.
[82]Uppal, R., and P. Caravan. Targeted probes for cardiovascular MRI. *Future Med. Chem*. 2:451–470, 2010.
[83]Veiseh, O., J. W. Gunn, and M. Q. Zhang. Design and fabrication of magnetic nanoparticles for targeted drug delivery and imaging. *Adv. Drug Deliv. Rev*. 62:284–304, 2010.
[84]Velde, G. V., V. Baekelandt, T. Dresselaers, and U. Himmelreich. Magnetic resonance imaging and spectroscopy methods for molecular imaging. *Q. J. Nucl. Med. Mol. Imaging* 53:565–585, 2009.
[85]Villaraza, A. J. L., A. Bumb, and M. W. Brechbiel. Macromolecules, dendrimers, and nanomaterials in magnetic resonance imaging: the interplay between size, function, and pharmacokinetics. *Chem. Rev*. 110:2921–2959, 2010.
[86]Weissleder, R., and M. J. Pittet. Imaging in the era of molecular oncology. *Nature* 452:580–589, 2008.
[87]Werner, E. J., A. Datta, C. J. Jocher, and K. N. Raymond. High-relaxivity MRI contrast agents: where coordination chemistry meets medical imaging. *Angew. Chem. Int. Ed*. 47:8568–8580, 2008.
[88]Winter, P. M., S. D. Caruthers, G. M. Lanza, and S. A. Wickline. Quantitative cardiovascular magnetic resonance for molecular imaging. *J. Cardiovasc. Magn. Reson*. 12:62, 2010.
[89]Yuan, W. F., L. Sun, H. H. Tang, Y. Q. Wen, G. Jiang, W. Huang, L. Jiang, Y. L. Song, H. Tian, and D. B. Zhu. A novel thermally stable spironaphthoxazine and its application in rewritable high density optical data storage. *Adv. Mater*. 17:156–160, 2005.
[90]Zhang, S. R., K. C. Wu, and A. D. Sherry. A novel pH-sensitive MRI contrast agent. *Angew. Chem. Int. Ed*. 38:3192–3194, 1999.
[91]Zhi, J. F., R. Baba, K. Hashimoto, and A. Fujishima. Photoelectrochromic properties of a spirobenzopyran derivative. *J. Photochem. Photobiol. A Chem*. 92:91–97, 1995.